Supplementary Materials for "New Tests for Equality of Several Covariance Functions for Functional Data"

Jia Guo, Bu Zhou, and Jin-Ting Zhang

S.1 ADDITIONAL SIMULATION RESULTS

S.1.1 Simulation 3: Constant common factor function

In Section 2.5, we pointed out that when there are no scale-differences in $\varpi_i[(s_1,t_1),(s_2,t_2)]$'s across different time points, the asymptotic powers of the quasi GPF test and the L^2-norm based test are comparable. It is then of interest how do GPF_{nv}, GPF_{rp} and $F_{\max,rp}$ perform against L^2_{br}, L^2_{rp} and $T_{\max,rp}$ when the common factor function is a constant. In this simulation study, we aim to compare GPF_{nv}, GPF_{rp} and $F_{\max,rp}$ against L^2_{br}, L^2_{rp} and $T_{\max,rp}$ under the data generating model (50) with $h(t)=1$. Tables S.1 and S.2 present the empirical sizes and powers (in percent) of L^2_{br} (L^2_{rp}), $T^2_{\max,rp}$, GPF_{nv}, GPF_{rp} and $F_{\max,rp}$ when the k functional samples follow Gaussian and non-Gaussian distributions, respectively. Similar to Simulation 2, in Table S.1 we only present the results of L^2_{br} while in Table S.2 we only present the results of L^2_{rp}.

First of all, it is seen that in terms of size control, both $F_{\max,rp}$ and $T_{\max,rp}$ have better performance under various simulation configurations with most of their empirical sizes close

Table S.1: Empirical sizes and powers (in percent) of the tests when $z_{ijr},\ r = 1, \ldots, q;\ j = 1, \ldots, n_i;\ i = 1, \ldots, k$ are i.i.d. $\mathcal{N}(0, 1)$ for Simulation 3.

ρ		$\mathbf{n}_1 = (20, 30, 30)$					$\mathbf{n}_2 = (30, 40, 50)$					$\mathbf{n}_3 = (80, 70, 100)$				
	ω	***0***	*1*	*2*	*3*	*6*	***0***	*1*	*1.5*	*2*	*3*	***0***	*0.5*	*1*	*1.5*	*2*
	L_{br}^2	**4.55**	10.91	54.61	90.22	99.99	**4.63**	15.89	45.56	77.89	99.01	**4.68**	7.94	37.32	87.38	99.42
	$T_{\max,rp}$	**5.58**	19.07	60.55	87.40	99.41	**5.26**	28.94	58.94	83.18	98.64	**5.15**	18.93	66.57	96.22	99.81
0.1	GPF_{nv}	**6.56**	11.87	51.53	86.03	99.17	**5.95**	14.74	41.08	72.00	97.85	**5.57**	7.85	32.99	81.63	98.80
	GPF_{rp}	**5.52**	9.93	49.44	85.66	99.56	**5.27**	13.38	39.53	70.68	97.88	**5.17**	7.46	32.22	81.03	98.73
	$F_{\max,rp}$	**5.35**	13.95	51.75	85.33	99.53	**5.22**	20.25	47.17	75.49	98.06	**4.95**	13.98	54.35	92.32	99.63
	ω	***0***	*0.5*	*1*	*1.5*	*2*	***0***	*0.4*	*0.8*	*1*	*1.2*	***0***	*0.3*	*0.4*	*0.5*	*0.7*
	L_{br}^2	**4.80**	23.24	74.56	96.42	99.65	**4.77**	24.47	80.66	93.48	98.31	**5.04**	36.64	62.49	83.95	98.65
	$T_{\max,rp}$	**5.55**	20.07	55.46	81.58	93.45	**5.51**	20.76	61.83	79.67	90.41	**5.17**	33.94	53.31	72.11	95.14
0.5	GPF_{nv}	**7.39**	25.72	72.05	93.31	98.23	**6.53**	23.64	75.57	90.92	97.13	**5.83**	31.56	55.78	78.22	98.32
	GPF_{rp}	**5.79**	21.31	68.61	93.22	98.69	**5.38**	20.53	72.84	89.74	96.83	**5.21**	29.38	53.07	76.37	98.10
	$F_{\max,rp}$	**5.62**	18.71	58.46	89.05	97.57	**5.50**	19.08	63.03	82.30	93.79	**5.25**	27.62	47.88	70.42	95.89
	ω	***0***	*0.5*	*0.8*	*1*	*1.5*	***0***	*0.4*	*0.5*	*0.7*	*1*	***0***	*0.2*	*0.3*	*0.4*	*0.5*
	L_{br}^2	**4.78**	34.87	71.73	89.47	99.58	**5.07**	32.68	52.41	85.68	99.23	**5.01**	19.88	48.49	79.40	95.72
	$T_{\max,rp}$	**5.40**	11.10	25.70	36.90	67.57	**5.57**	10.78	15.61	29.44	58.32	**5.28**	8.54	15.32	27.00	44.33
0.9	GPF_{nv}	**8.28**	35.68	74.14	89.69	98.87	**6.41**	33.32	51.94	83.85	98.90	**5.60**	19.41	46.72	77.02	94.63
	GPF_{rp}	**8.10**	34.00	72.24	88.09	98.93	**6.69**	32.98	51.05	82.96	98.70	**5.87**	20.48	47.38	77.36	94.67
	$F_{\max,rp}$	**5.91**	12.83	27.73	44.05	82.71	**5.45**	12.46	18.01	33.67	68.29	**5.41**	9.51	17.67	30.73	49.95

Table S.2: Empirical sizes and powers (in percent) of the tests when $z_{ijr},\ r = 1, \ldots, q;\ j = 1, \ldots, n_i;\ i = 1, \ldots, k$ are i.i.d. $(3/5)^{1/2} t_5$ for Simulation 3.

ρ		$\mathbf{n}_1 = (20, 30, 30)$					$\mathbf{n}_2 = (30, 40, 50)$					$\mathbf{n}_3 = (80, 70, 100)$				
	ω	***0***	*2*	*2.6*	*3.8*	*12*	***0***	*1.5*	*2.2*	*3*	*5*	***0***	*1.2*	*1.5*	*1.8*	*2.6*
	L^2_{rp}	**5.86**	37.28	56.01	79.14	94.39	**5.49**	29.20	61.14	83.10	96.52	**5.04**	37.96	61.62	79.46	97.18
	$T_{\max,rp}$	**5.80**	40.20	56.33	76.17	93.28	**5.67**	38.15	65.35	83.14	95.25	**5.36**	59.27	77.92	89.28	98.32
0.1	GPF_{nv}	**5.12**	33.87	52.43	74.34	88.98	**4.95**	24.91	55.30	78.62	92.72	**4.65**	30.99	53.97	73.08	95.09
	GPF_{rp}	**5.74**	34.98	54.73	78.92	94.46	**5.51**	26.07	58.42	82.54	96.68	**5.12**	33.00	56.17	75.53	96.73
	$F_{\max,rp}$	**5.60**	36.87	54.99	78.87	94.91	**5.59**	31.38	61.54	83.28	96.81	**5.19**	49.84	70.92	85.12	97.97
	ω	***0***	*0.8*	*1.1*	*1.5*	*5*	***0***	*0.6*	*0.8*	*1.1*	*1.8*	***0***	*0.4*	*0.5*	*0.7*	*1*
	L^2_{rp}	**6.01**	36.76	57.16	75.09	94.35	**5.50**	34.03	52.64	74.87	93.82	**5.10**	37.43	56.20	83.18	96.71
	$T_{\max,rp}$	**5.56**	25.61	41.03	57.05	90.74	**5.12**	25.73	38.07	57.67	85.27	**5.12**	35.18	48.96	74.36	93.22
0.5	GPF_{nv}	**5.56**	36.72	57.48	73.74	89.50	**4.96**	29.93	49.93	72.83	91.15	**4.43**	28.03	46.17	76.44	94.37
	GPF_{rp}	**5.99**	36.76	58.65	76.98	94.78	**5.46**	31.23	51.56	75.35	94.71	**5.42**	30.88	49.31	79.27	95.95
	$F_{\max,rp}$	**5.77**	31.82	52.86	73.47	95.39	**5.43**	29.11	46.87	72.05	94.46	**5.31**	33.71	51.41	80.46	96.80
	ω	***0***	*0.6*	*0.8*	*1.1*	*1.8*	***0***	*0.5*	*0.6*	*0.8*	*1.2*	***0***	*0.3*	*0.4*	*0.5*	*0.7*
	L^2_{rp}	**8.35**	32.16	48.88	70.14	88.63	**6.83**	31.92	44.39	69.33	90.26	**5.87**	29.85	55.11	76.08	95.60
	$T_{\max,rp}$	**5.61**	10.75	17.01	28.28	55.71	**5.58**	10.61	13.63	24.07	50.29	**5.33**	11.25	18.85	29.31	56.02
0.9	GPF_{nv}	**5.06**	27.49	46.93	71.08	88.07	**3.98**	25.64	38.26	67.51	90.23	**3.03**	20.16	43.41	67.13	92.66
	GPF_{rp}	**8.53**	33.89	53.78	75.82	92.58	**7.03**	33.23	46.60	73.97	93.73	**5.84**	29.39	54.85	76.71	96.56
	$F_{\max,rp}$	**6.35**	14.37	22.04	39.75	78.76	**5.96**	14.10	18.52	32.32	68.21	**5.56**	13.38	22.57	33.82	66.74

to the nominal size 5%. GPF_{nv} and GPF_{rp} perform well when the functional data are highly correlated or when the sample sizes are large. On the other hand, L^2_{br} performs quite well under the Gaussian case, L^2_{rp} performs well when the functional data are highly correlated or the sample sizes are large but it is liberal when the functional data are less correlated or when the sample sizes are too small. In terms of power, it seems GPF_{nv}, GPF_{rp} and L^2_{br} (L^2_{rp}) have comparable powers but they have smaller (or higher) powers than $F_{\max,rp}$ and $T_{\max,rp}$ when the functional data are highly (or less) correlated.

S.1.2 Simulation 4: Monotonically increasing common factor function

In the two simulation studies in the main paper, the common factor function $h(t)$ is monotonically decreasing. In this simulation study, we aim to compare GPF_{nv}, GPF_{rp} and $F_{\max,rp}$ against L^2_{rp} and $T_{\max,rp}$ under the data generating model (50) with $h(t) = (t+1/J)$, which is a monotonically increasing function. Table S.3 presents the empirical sizes and powers (in percent) of L^2_{rp}, $T_{\max,rp}$, GPF_{nv}, GPF_{rp} and $F_{\max,rp}$ when the k functional samples follow Gaussian distributions. From Table S.3, it is seen that similar to Simulation 2, GPF_{nv}, GPF_{rp} and $F_{\max,rp}$ are significantly more powerful than L^2_{rp} and $T^2_{\max,rp}$. Although $F_{\max,rp}$ is less powerful than GPF_{nv} and GPF_{rp} when $\rho = 0.9$ and $\boldsymbol{n} = \boldsymbol{n}_1, \boldsymbol{n}_2$, it is generally more powerful than GPF_{nv} and GPF_{rp} in all the other cases. These conclusions are consistent with those we drawn from Simulation 2 in the main paper.

Table S.3: Empirical sizes and powers (in percent) of L^2_{rp}, $T_{\max}$, GPF_{nv}, GPF_{rp} and $F_{\max,rp}$ when $z_{ijr}, r = 1, \ldots, q; j = 1, \ldots, n_i; i = 1, \ldots, k$ are i.i.d. $\mathcal{N}(0, 1)$ for Simulation 4.

ρ		$\mathbf{n}_1 = (20, 30, 30)$			$\mathbf{n}_2 = (30, 40, 50)$			$\mathbf{n}_3 = (80, 70, 100)$		
	ω	***0***	*0.035*	*0.3*	***0***	*0.026*	*0.045*	***0***	*0.0176*	*0.024*
	L^2_{rp}	**5.22**	5.47	6.20	**5.03**	4.94	5.58	**4.82**	5.02	5.34
	$T_{\max}$	**5.28**	5.72	5.92	**5.26**	5.03	5.61	**4.97**	4.59	5.09
0.1	GPF_{nv}	**6.33**	6.51	15.63	**5.88**	5.73	6.57	**5.18**	5.08	5.47
	GPF_{rp}	**5.29**	5.39	12.56	**5.09**	5.05	5.81	**5.04**	4.75	5.21
	$F_{\max,rp}$	**5.53**	54.75	96.55	**5.46**	54.02	95.16	**5.16**	57.19	95.56
	ω	***0***	*0.028*	*0.6*	***0***	*0.018*	*0.14*	***0***	*0.009*	*0.015*
	L^2_{rp}	**6.08**	6.01	87.28	**5.56**	5.69	10.60	**5.10**	5.36	5.83
	$T_{\max}$	**5.98**	5.85	21.05	**5.16**	5.42	6.49	**5.11**	4.91	5.16
0.5	GPF_{nv}	**7.87**	10.91	94.79	**6.58**	9.19	58.48	**6.24**	7.52	10.53
	GPF_{rp}	**6.16**	8.25	94.48	**5.38**	7.59	54.45	**5.55**	6.82	9.58
	$F_{\max,rp}$	**5.71**	52.80	92.49	**5.25**	54.09	98.32	**5.33**	52.79	97.17
	ω	***0***	*0.1*	*0.35*	***0***	*0.06*	*0.25*	***0***	*0.02*	*0.028*
	L^2_{rp}	**6.62**	8.85	30.90	**5.96**	7.17	21.96	**5.32**	5.90	6.43
	$T_{\max}$	**5.76**	5.99	7.23	**5.50**	5.80	6.45	**5.28**	5.23	5.28
0.9	GPF_{nv}	**8.01**	46.67	94.07	**6.43**	37.28	98.09	**5.31**	20.48	36.87
	GPF_{rp}	**7.79**	44.80	94.13	**6.81**	37.21	98.10	**5.91**	21.39	38.26
	$F_{\max,rp}$	**6.10**	55.83	70.69	**5.69**	77.57	94.07	**5.52**	63.70	95.47

S.1.3 Simulation 5: On the choice of basis functions

In Simulation 1, we used a BIC criterion to select the number of Fourier basis functions for estimating the functional principal components in the implementation of $FSHK_1$ and $FSHK_2$. It is of interest if the choice of the number of basis functions involved and the choice of bases have a strong impact on the performance of these two tests. In this simulation study, we consider using different number of basis functions $L = 11, 21, 41, 81$ and also consider using B-spline basis functions. To save computation, the number of simulation repetitions is reduced to $N = 1000$. The results using different number of Fourier basis functions to estimate the functional principal components in $FSHK_1$ and $FSHK_2$ are presented in Table S.4 where the cases $\boldsymbol{n} = (30, 40)$ and some choices of ω are omitted for space saving.

It can be seen from Table S.4 that $FSHK_1$ and $FSHK_2$ have comparable performance for different number of basis functions, and are again less powerful than GPF_{nv}, GPF_{rp} and $F_{\max}$ (see the results in Table 1 of the main paper). The results using B-spline basis functions are presented in Table S.5, where the cases $\rho = 0.5$ and $\boldsymbol{n} = (30, 40)$ are omitted for space saving. It is seen from Table S.5 that the tests $FSHK_1$ and $FSHK_2$ perform comparably for different L, and similar conclusions can be drawn as those drawn from Simulation 1 of the main paper.

Table S.4: Empirical sizes and powers (in percentages) of FSHK_1 and FSHK_2 when $z_{ijr}, r = 1, \ldots, q; j = 1, \ldots, n_i; i = 1, \ldots, k$ are i.i.d. $\mathcal{N}(0, 1)$ using Fourier basis functions for Simulation 5.

L	ρ		$\mathbf{n}_1 = (20, 30)$			$\mathbf{n}_3 = (80, 70)$			L	$\mathbf{n}_1 = (20, 30)$			$\mathbf{n}_3 = (80, 70)$		
		ω	***0***	*8*	*14*	***0***	*3.5*	*5*		***0***	*8*	*14*	***0***	*3.5*	*5*
	0.1	FSHK_1	**6.7**	9.2	55.8	**5.8**	4.8	5.1		**7.7**	9.3	58.4	**5.5**	5.9	4.6
		FSHK_2	**5.2**	7.7	51.6	**5.4**	5.6	6.1		**6.2**	7.5	56.3	**5.4**	5.9	5.3
		ω	***0***	*3*	*6*	***0***	*1.4*	*2*		***0***	*3*	*6*	***0***	*1.4*	*2*
11	0.5	FSHK_1	**8.3**	33.1	84.4	**5.7**	9.1	19.3	21	**7.5**	31.7	84.9	**5.0**	9.3	17.8
		FSHK_2	**3.4**	15.6	73.5	**5.7**	13.9	25.0		**5.3**	13.4	74.5	**5.3**	13.3	23.9
		ω	***0***	*2.2*	*4*	***0***	*1.1*	*1.7*		***0***	*2.2*	*4*	***0***	*1.1*	*1.7*
	0.9	FSHK_1	**9.5**	15.2	36.4	**4.2**	4.5	6.4		**9.0**	16.9	34.0	**4.0**	6.1	6.7
		FSHK_2	**4.6**	4.9	12.4	**5.0**	5.3	8.3		**5.5**	4.8	13.0	**4.6**	5.8	7.7
		ω	***0***	*8*	*14*	***0***	*3.5*	*5*		***0***	*8*	*14*	***0***	*3.5*	*5*
	0.1	FSHK_1	**6.4**	9.3	55.3	**5.5**	6.3	4.9		**7.3**	11.3	57.3	**5.2**	4.9	5.2
		FSHK_2	**4.7**	6.0	52.6	**5.6**	6.1	5.4		**5.0**	8.4	53.6	**5.3**	5.3	5.4
		ω	***0***	*3*	*6*	***0***	*1.4*	*2*		***0***	*3*	*6*	***0***	*1.4*	*2*
41	0.5	FSHK_1	**9.6**	31.0	85.4	**5.0**	11.2	20.8	81	**6.7**	31.3	85.0	**5.1**	10.8	20.0
		FSHK_2	**4.8**	16.4	73.6	**4.9**	14.6	26.0		**4.8**	13.9	71.5	**5.0**	14.2	26.8
		ω	***0***	*2.2*	*4*	***0***	*1.1*	*1.7*		***0***	*2.2*	*4*	***0***	*1.1*	*1.7*
	0.9	FSHK_1	**10.1**	15.6	34.9	**4.6**	4.8	6.1		**9.1**	15.6	36.4	**5.1**	5.0	6.2
		FSHK_2	**4.9**	4.0	10.8	**4.6**	6.0	8.9		**5.5**	4.9	14.1	**5.3**	5.9	7.4

Table S.5: Empirical sizes and powers (in percent) of FSHK_1, FSHK_2, GPF_{nv}, GPF_{rp} and $F_{\max,rp}$ when $z_{ijr}, r = 1, \ldots, q; j = 1, \ldots, n_i; i = 1, \ldots, k$ are i.i.d. $\mathcal{N}(0,1)$ using B-spline basis functions for Simulation 5.

L	ρ		$\mathbf{n}_1 = (20,30)$			$\mathbf{n}_3 = (80,70)$			L	$\mathbf{n}_1 = (20,30)$			$\mathbf{n}_3 = (80,70)$		
		ω	***0***	*8*	*14*	***0***	*3.5*	*5*		***0***	*8*	*14*	***0***	*3.5*	*5*
		FSHK_1	**5.6**	7.4	52.5	**4.7**	4.4	5.3		**7.8**	8.3	57.9	**5.3**	5.8	5.4
		FSHK_2	**4.6**	6.2	50.3	**4.6**	4.9	5.6		**5.9**	5.6	56.8	**5.3**	5.5	6.1
	0.1	GPF_{nv}	**6.2**	53.8	91.0	**5.0**	24.6	64.5		**6.2**	48.9	90.9	**5.0**	25.1	66.1
		GPF_{rp}	**5.2**	50.8	92.2	**5.1**	24.0	63.2		**4.8**	44.6	91.8	**4.9**	24.7	65.4
11		$F_{\max,rp}$	**4.9**	76.0	91.6	**5.4**	83.1	99.7	21	**5.0**	73.6	91.4	**5.3**	85.1	99.9
		ω	***0***	*2.2*	*4*	***0***	*1.1*	*1.7*		***0***	*2.2*	*4*	***0***	*1.1*	*1.7*
		FSHK_1	**9.6**	9.3	15.2	**5.1**	4.1	4.4		**8.9**	12.2	20.5	**5.8**	5.0	4.2
		FSHK_2	**5.6**	4.9	6.6	**5.0**	4.6	4.7		**4**	4.1	8.6	**5.5**	5.3	6.2
	0.9	GPF_{nv}	**5.1**	47.3	91.4	**3.9**	50.2	91.5		**5**	43.6	92.4	**4.3**	50.5	90.4
		GPF_{rp}	**7.3**	52.2	92.1	**5.2**	57.1	93.7		**7**	49.1	93.2	**5.9**	57.1	92.2
		$F_{\max,rp}$	**5.7**	16.7	47.4	**4.7**	23.3	49.2		**5.6**	16.0	50.5	**5.6**	21.8	50.2
		ω	***0***	*8*	*14*	***0***	*3.5*	*5*		***0***	*8*	*14*	***0***	*3.5*	*5*
		FSHK_1	**6.9**	8.6	61.7	**5.3**	4.8	5.2		**6**	6.5	58.5	**4.4**	5.4	5.0
		FSHK_2	**5.9**	6.3	60.2	**5.5**	5.1	5.1		**4.8**	4.1	56.6	**4.9**	5.6	5.4
	0.1	GPF_{nv}	**6.3**	50.6	92.7	**5.4**	27.5	64.0		**6.3**	52.5	90.5	**5.3**	27.7	61.6
		GPF_{rp}	**5.0**	47.7	93.7	**5**	26.8	64.2		**5.1**	47.9	91.4	**5.1**	26.8	61.3
41		$F_{\max,rp}$	**4.9**	72.9	90.9	**5.2**	82.7	99.7	81	**5.2**	74.1	89.3	**5.3**	85.6	99.7
		ω	***0***	*2.2*	*4*	***0***	*1.1*	*1.7*		***0***	*2.2*	*4*	***0***	*1.1*	*1.7*
		FSHK_1	**9.3**	12.6	22.7	**5.0**	5.2	4.3		**8.5**	13.0	20.5	**4.8**	4.5	5.7
		FSHK_2	**5.3**	4.1	8.6	**5.6**	5.1	5.9		**4.8**	4.7	6.8	**5.1**	4.8	5.8
	0.9	GPF_{nv}	**4.1**	46.2	90.9	**4.3**	52.8	90.6		**4.8**	45.1	90.5	**4.2**	50.9	90.4
		GPF_{rp}	**7.1**	50.7	92.3	**6.2**	58.8	92.8		**7.1**	51.3	92.1	**5.9**	59.0	92.9
		$F_{\max,rp}$	**6.3**	16.5	46.0	**5.8**	22.6	50.2		**4.6**	17.6	45.0	**5.6**	22.2	53.6

S.1.4 Simulation 6: On the number of permutations

In the previous simulation studies, we used the number of permutations $P = 1000$ for L_{rp}^2, $T_{\max}$, GPF_{rp} and $F_{\max}$. A larger number of P may be desired but is often limited by the computational cost. To examine the effect of the number of permutations P and the time used for the implementation, we repeat two simulation cases of Simulations 2 and 3, respectively, with different numbers of permutations $P = 200, 500, 1000, 2000$ and present the results in Tables S.6 and S.7, respectively.

From Tables S.6 and S.7, it is seen that L_{rp}^2, $T_{\max}$, GPF_{rp} and $F_{\max}$ have comparable empirical sizes and powers for different P. One possible explanation is the considered P's are not large enough to observe a significant impact of the number of permutations. However, increasing the number of permutations often means the time used increases substantially.

Table S.6: Empirical sizes and powers (in percent) of the tests and the time used for different number of permutations under the settings of Simulation 2 when $\rho = 0.5$, $\boldsymbol{n} = (30, 40, 50)$, $z_{ijr}, r = 1, \ldots, q; j = 1, \ldots, n_i; i = 1, \ldots, k$ are i.i.d. $\mathcal{N}(0, 1)$ for Simulation 6.

$P = 200$, Time=56.72 minutes						$P = 500$, Time=2.19 hours				
ω	***0***	*0.8*	*1.2*	*1.5*	*2*	***0***	*0.8*	*1.2*	*1.5*	*2*
L^2_{rp}	**5.57**	5.14	5.51	5.53	5.20	**5.25**	5.04	5.58	5.27	5.36
$T_{max,rp}$	**5.45**	5.32	5.37	5.44	5.03	**5.28**	5.15	5.52	5.17	5.26
GPF_{nv}	**6.43**	29.17	57.40	76.47	94.07	**6.91**	30.27	57.27	76.04	94.06
GPF_{rp}	**5.20**	25.11	52.21	72.53	93.03	**5.55**	26.35	52.92	73.11	93.31
$F_{\max,rp}$	**5.45**	33.21	63.83	81.66	95.56	**5.77**	33.97	63.88	82.14	95.62
$P = 1000$, Time=4.28 hours						$P = 2000$, Time=8.44 hours				
ω	***0***	*0.8*	*1.2*	*1.5*	*2*	***0***	*0.8*	*1.2*	*1.5*	*2*
L^2_{rp}	**5.47**	5.53	5.43	5.19	5.35	**5.02**	5.33	5.37	5.02	5.14
$T_{max,rp}$	**5.42**	5.45	5.33	5.11	5.31	**5.11**	5.39	5.43	4.83	4.94
GPF_{nv}	**6.73**	30.55	56.85	76.49	94.20	**6.28**	29.16	57.18	76.74	94.84
GPF_{rp}	**5.47**	26.68	52.52	73.44	93.55	**5.31**	25.63	52.83	74.07	94.33
$F_{\max,rp}$	**5.75**	34.93	63.80	82.42	95.89	**5.38**	33.79	64.37	83.08	96.39

Table S.7: Empirical sizes and powers (in percent) of the tests and the time used for different number of permutations under the settings of Simulation 3 when $\rho = 0.9$, $\boldsymbol{n} = (80, 70, 100)$, $z_{ijr}, r = 1, \ldots, q; j = 1, \ldots, n_i; i = 1, \ldots, k$ are i.i.d. $(3/5)^{1/2} t_5$ for Simulation 6.

$P = 200$, Time=2.14 hours						$P = 500$, Time=4.62 hours				
ω	***0***	*0.3*	*0.4*	*0.5*	*0.7*	***0***	*0.3*	*0.4*	*0.5*	*0.7*
L^2_{rp}	**6.38**	29.76	54.26	75.65	95.15	**5.66**	3.02	5.48	76.3	95.18
$T_{max,rp}$	**5.52**	10.92	18.88	28.97	54.87	**5.63**	11.70	18.72	28.53	55.52
GPF_{nv}	**3.16**	19.84	42.27	66.28	92.57	**2.85**	20.02	43.13	66.83	92.38
GPF_{rp}	**6.54**	28.94	53.70	76.37	96.31	**5.66**	29.50	54.37	77.33	96.38
$F_{\max,rp}$	**5.48**	13.15	21.65	34.18	66.32	**5.05**	14.51	22.32	34.39	66.90
$P = 1000$, Time=8.75 hours						$P = 2000$, Time=17.03 hours				
ω	***0***	*0.3*	*0.4*	*0.5*	*0.7*	***0***	*0.3*	*0.4*	*0.5*	*0.7*
L^2_{rp}	**5.47**	29.73	54.45	76.48	95.45	**5.98**	30.01	54.16	76.70	95.37
$T_{max,rp}$	**5.50**	11.92	18.97	28.81	56.69	**5.64**	11.77	19.07	29.79	57.16
GPF_{nv}	**3.08**	19.63	42.43	67.27	92.50	**3.14**	19.80	42.30	66.56	92.51
GPF_{rp}	**5.42**	29.20	53.97	77.33	96.44	**5.89**	29.21	53.62	77.25	96.35
$F_{\max,rp}$	**5.34**	13.36	22.20	35.00	67.22	**5.44**	13.79	22.29	35.43	66.44

S.1.5 Simulation 7: On the exchangeability

At the end of Section 2.3, we mentioned that the performance of the random permutation method relies on the exchangeability of the permuted data. It is of interest if the violation of this exchangeability will have a strong impact on the performance of the random permutation based approaches. In this simulation study, we use the same simulation settings as in Simulation 1 of the main paper, but let the first group sample be i.i.d Gaussian and the second group sample be i.i.d non-Gaussian via setting $z_{1jr}, r = 1, \ldots, q; j = 1, \ldots, n_1 \overset{i.i.d.}{\sim} \mathcal{N}(0, 1)$ and $z_{2jr}, r = 1, \ldots, q; j = 1, \ldots, n_2 \overset{i.i.d.}{\sim} (3/5)^{1/2} t_5$. In this way, the samples of the two groups still have the same covariance function under the null hypothesis but have different higher order moment functions. It is said that Assumption A3 in the main paper is violated and the samples of the two groups are not exchangeable. Empirical sizes and powers of the random permutation based tests L^2_{rp}, $T_{\max}$, GPF_{rp}, $F_{\max,rp}$, and the Welch–Satterthwaite approximation based test GPF_{nv} are presented in Table S.8. It is seen that all the random permutation based tests are very liberal and their empirical sizes are generally larger than those presented in Simulations 1 and 2 of the main paper. GPF_{nv} is liberal when $\rho = 0.1, 0.5$ but becomes conservative when $\rho = 0.9$. It seems that L^2_{rp}, $T_{\max,rp}$ are less liberal than GPF_{rp} and $F_{\max,rp}$. This simulation shows that GPF_{nv}, GPF_{rp} and $F_{\max,rp}$ may not have a good size control when Assumption A3 is not satisfied.

Table S.8: Empirical sizes and powers (in percent) of L^2_{rp}, $T_{\max}$, GPF_{nv}, GPF_{rp} and $F_{\max,rp}$ when $z_{1jr}, r = 1, \ldots, q; j = 1, \ldots, n_1$ are i.i.d. $\mathcal{N}(0,1)$ and $z_{2jr}, r = 1, \ldots, q; j = 1, \ldots, n_2$ are i.i.d. $(3/5)^{1/2} t_5$ for Simulation 7.

ρ		$\mathbf{n}_1 = (20, 30, 30)$					$\mathbf{n}_2 = (30, 40, 50)$					$\mathbf{n}_3 = (80, 70, 100)$				
	ω	***0***	*8*	*11*	*15*	*28*	***0***	*6*	*8*	*11*	*15*	***0***	*5*	*6*	*7*	*10*
	L^2_{rp}	**6.59**	6.93	6.20	6.63	19.67	**6.90**	6.38	6.37	6.69	7.22	**7.28**	7.01	7.30	7.55	7.07
	$T_{\max,rp}$	**6.70**	6.86	6.81	6.93	6.40	**6.98**	6.65	6.71	6.93	6.74	**7.24**	7.16	7.60	7.77	7.05
0.1	GPF_{nv}	**7.45**	29.82	53.40	72.75	84.40	**7.46**	23.79	49.82	78.55	88.41	**7.40**	43.38	67.85	86.30	98.30
	GPF_{rp}	**6.70**	28.64	55.00	77.68	91.52	**7.08**	24.26	52.25	83.71	95.11	**7.57**	46.02	71.15	89.42	99.93
	$F_{\max,rp}$	**7.21**	49.74	60.72	67.44	71.28	**7.20**	63.33	78.95	84.83	86.20	**7.52**	96.24	97.78	98.26	98.51
	ω	***0***	*3*	*4*	*8*	*15*	***0***	*2*	*3*	*4*	*7*	***0***	*1.4*	*1.9*	*2.5*	*3.8*
	L^2_{rp}	**5.53**	5.71	5.72	6.17	21.79	**6.25**	5.81	5.40	5.75	6.44	**6.20**	6.07	6.00	6.02	6.11
	$T_{\max,rp}$	**5.75**	5.74	5.90	5.77	5.37	**6.08**	5.87	5.62	5.84	5.85	**6.03**	6.17	6.05	5.88	5.91
0.5	GPF_{nv}	**7.47**	33.14	49.12	79.51	85.92	**6.49**	29.81	51.70	71.43	91.43	**6.85**	43.39	69.92	87.84	98.08
	GPF_{rp}	**6.95**	31.51	49.34	86.81	93.00	**6.52**	30.07	53.48	76.18	97.58	**7.55**	46.01	73.07	91.14	99.69
	$F_{\max,rp}$	**6.93**	38.03	49.64	65.74	70.79	**6.75**	43.49	63.55	78.52	87.60	**6.47**	63.79	86.90	96.63	98.95
	ω	***0***	*2*	*3*	*4*	*8*	***0***	*1.6*	*2.2*	*3*	*5*	***0***	*0.9*	*1.4*	*1.7*	*3*
	L^2_{rp}	**5.32**	5.47	5.18	5.27	5.35	**5.39**	5.76	5.60	5.49	5.19	**5.61**	5.46	5.67	5.59	5.25
	$T_{\max,rp}$	**5.30**	5.39	5.50	5.25	5.21	**5.48**	5.44	5.49	5.29	5.10	**5.55**	5.54	5.65	5.69	5.16
0.9	GPF_{nv}	**3.32**	20.86	44.15	67.03	85.31	**2.65**	23.46	43.84	71.15	91.85	**2.88**	22.49	57.60	77.66	98.55
	GPF_{rp}	**6.57**	29.52	52.93	74.44	92.75	**5.94**	36.69	58.73	82.88	97.78	**6.71**	35.90	72.83	88.45	99.93
	$F_{\max,rp}$	**6.77**	14.30	21.67	33.78	61.60	**6.22**	17.24	25.30	41.01	79.56	**6.14**	16.50	32.13	45.75	93.85

S.2 Graphical illustration of the simulated function data

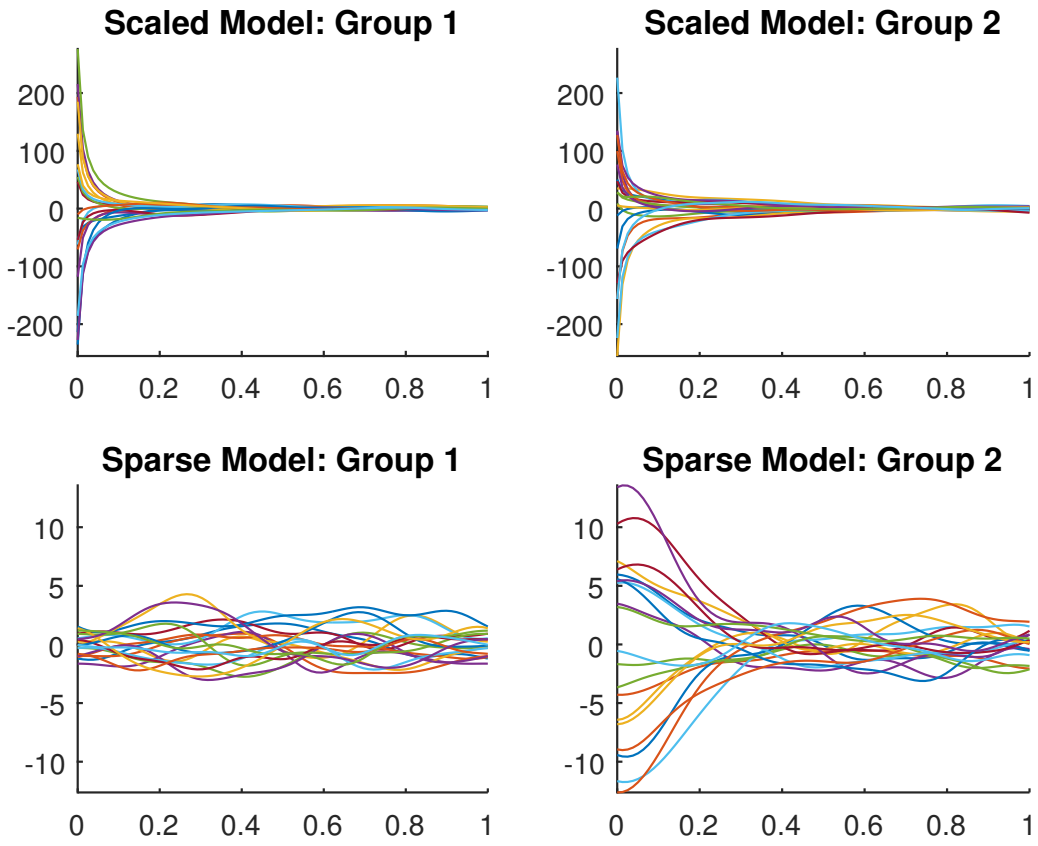

Figure S.1: The simulated functional data (different samples/curves are in different colors).

At the end of Simulation 2 of the main paper, we mentioned that $T_{\max,rp}$ and $F_{\max,rp}$ performed differently in Simulation 2 and in the paper by Guo et al. (2018) because the simulated models under consideration are different. The simulated model used in the main

paper may be referred to as the scaled model while the simulated model used in Guo et al. (2018) may be referred to as the sparse model. In this section, we give a graphical illustration of the simulated data generated from these two different models. The simulated functional data generated using the scaled model in Simulations 1 and 2 of the main paper and those generated using the sparse model of Guo et al. (2018) are presented in Figure S.1. For space saving, only two groups of functional data with $\omega = 4$, $\rho = 0.5$ and $n_1 = n_2 = 20$ under the Gaussian case (when $z_{ijr},\ r = 1, \ldots, q;\ j = 1, \ldots, n_i;\ i = 1, \ldots, k$ are i.i.d. $\mathcal{N}(0, 1)$) are plotted.

S.3 Further studies on the medfly mortality data

S.3.1 Real-data based simulation: power comparison

In this simulation study, we used the medfly mortality data set given in Section 4 of the main paper to compare the powers of GPF_{nv}, GPF_{rp}, $F_{\max,rp}$, L^2_{br}, L^2_{rp} and $T_{\max,rp}$. To this end, we randomly resampled the survival functions with replacement from each of the four groups to form a bootstrap dataset, and applied all the tests to check if the four groups of the bootstrap dataset have the same covariance function. Note that conditionally on the original data, the four conditional covariance functions of the bootstrap dataset are the four sample covariance functions respectively presented in Figure 1 of the main paper, which are clearly different. We repeat the above bootstrap process $10,000$ times to calculate the empirical powers of the tests based on a given nominal size $\alpha \in [0, 0.1]$. The empirical powers vs α are plotted in Figure S.2. It is seen the supremum based tests such as $T_{\max,rp}$ and $F_{\max,rp}$ are more powerful than other tests, and the pointwise quasi F-statistic based tests $\mathrm{GPF}_{nv}, \mathrm{GPF}_{rp}$ and $F_{\max,rp}$ are generally more powerful than those L^2-norm based

tests L^2_{br} and L^2_{rp}. It is also seen that $F_{\max,rp}$ is the most powerful test among all the tests under consideration. These conclusions are consistent with those we observed from Table 5 of the main paper.

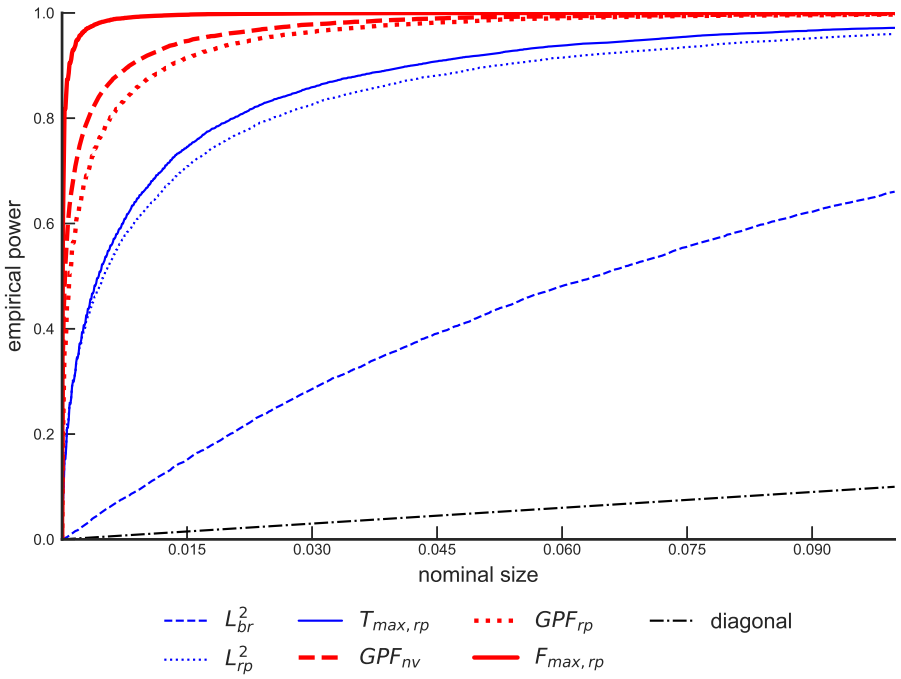

Figure S.2: Empirical powers of the tests for the medfly mortality data.

S.3.2 Real-data based simulation: size control comparison

Similarly, to study the size controls of these tests, we can bootstrap from the pooled samples of the four groups and generate a bootstrap dataset containing four groups. The empirical sizes vs α are plotted in Figure S.3. It is seen that the size controls of these tests are generally comparable, except L^2_{br} is rather conservative. It is also seen that $T_{\max,rp}$ has best

overall size control. GPF_{nv} is a little liberal, possibly because the group sample sizes are small. L^2_{br} did not work well, probably due to the serious violation of data Gaussianity.

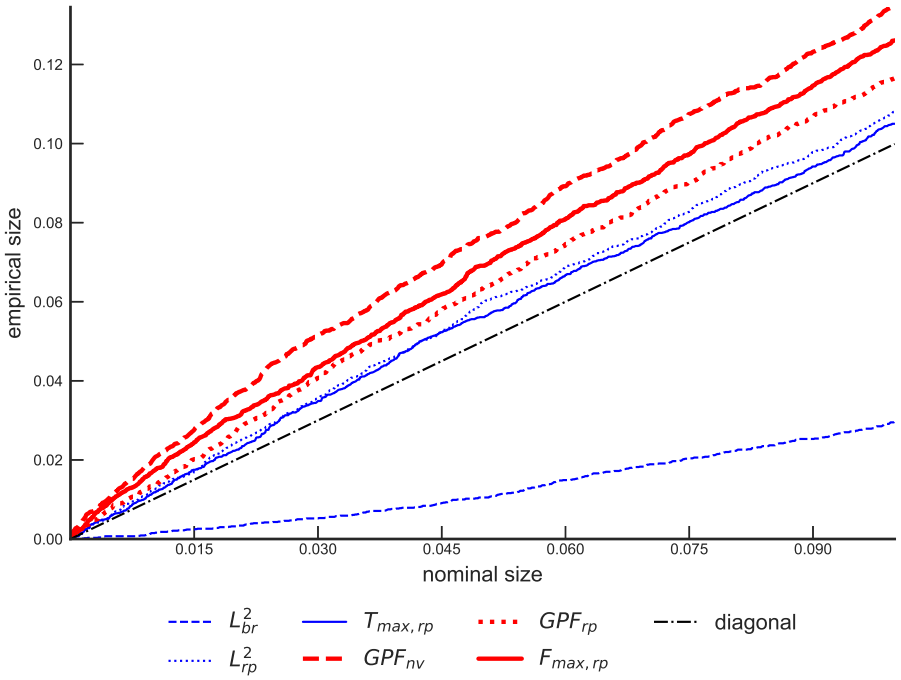

Figure S.3: Empirical sizes of the tests for the medfly mortality data.

S.3.3 Raw survival and sample mean survival functions

The usual life span of a medfly is short, only around 3–4 weeks (Carey et al. 2008). The raw and sample mean survival curves over the whole range are presented in Figures S.4 and S.5, respectively. It is seen that after the first 31 days, all the group sample mean survival functions are smaller than 0.05, and after the first 40 days, the values of the group sample mean survival functions are so small that they can be ignored.

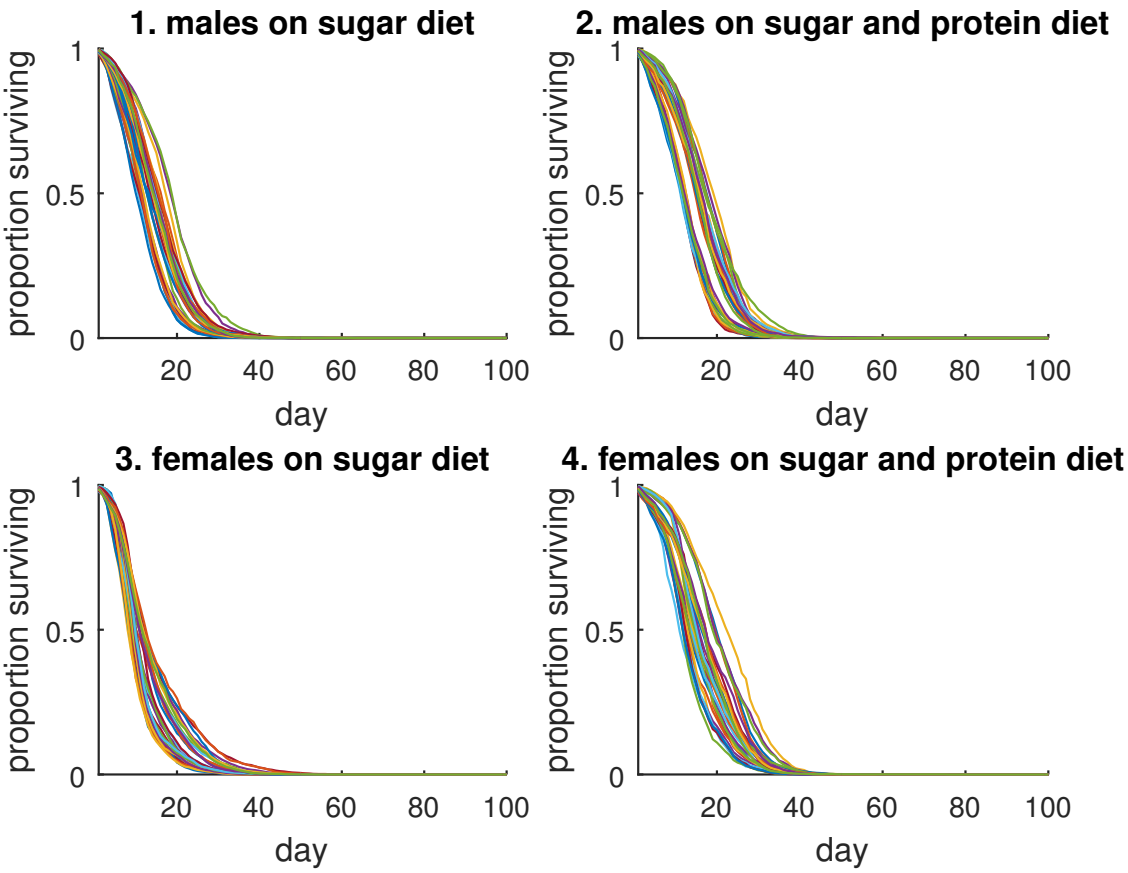

Figure S.4: The survival functions of the four medfly groups.

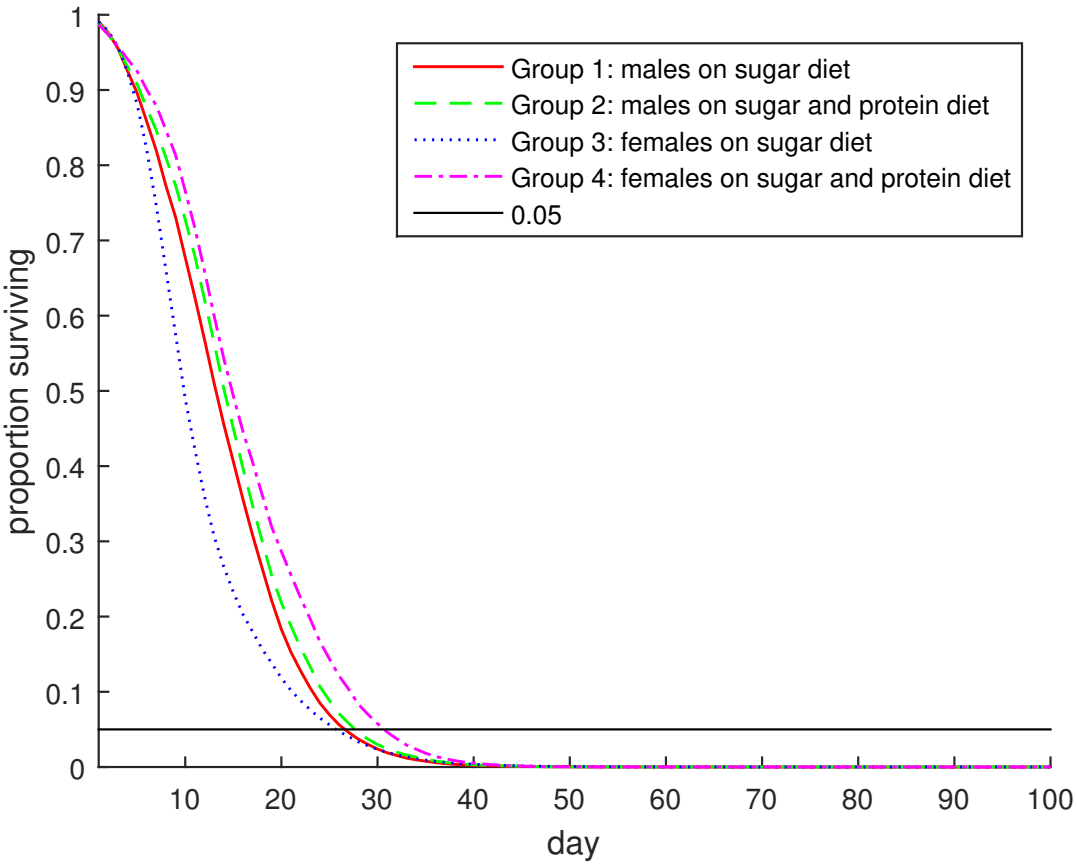

Figure S.5: The sample mean survival functions of the four medfly groups.

S.4 A note on the Welch–Satterthwaite χ^2-approximation

Zhang et al. (2017) provide a theoretical justification why the Welch–Satterthwaite χ^2-approximation is preferred to the widely-used normal approximation. For the normal approximation, we mean to approximate the distribution of T_0 using a normal distribution. Let $d^* = \frac{(k-1)\mathrm{tr}^2(\gamma_w^{\otimes 3})}{\mathrm{tr}^3(\gamma_w^{\otimes 2})}$ and $M = \frac{\mathrm{tr}(\gamma_w^{\otimes 4})}{(k-1)\mathrm{tr}^2(\gamma_w^{\otimes 2})}$, where $\gamma_w^{\otimes \ell}[(s_1,t_1),(s_2,t_2)] = \int_{\mathcal{T}^2} \gamma_w^{\otimes(\ell-1)}[(s_1,t_1),(u,v)]\gamma_w[(u,v),(s_2,t_2)]\mathrm{d}u\mathrm{d}v$, $\ell = 2,3,4,\ldots$. Then the skewness and kurtosis of T_0 can be expressed as $(8/d^*)^{1/2}$ and $12M$ respectively. It is easy to verify that $d^{-1} \leq (d^*)^{-1} \leq M$. It can be shown (see, e.g., Lemma 2 of Zhang et al. 2017) that the density error bound of the Welch–Satterthwaite χ^2-approximation is $O(M) + O(d^{-1}) + O[(d^*)^{-1/2} - d^{1/2}]$ which is much smaller than the density error bound of the associated normal approximation $O[(d^*)^{-1/2}]$ as given in Theorem 1 (a) of Zhang (2005). In addition, that the Welch–Satterthwaite χ^2-approximation approach enjoys both computational efficiency and good accuracy has been verified by a number of numerical applications and simulation studies conducted in the literature, including Satterthwaite (1946), Welch (1947), Guo et al. (2016) and recently by Zhang et al. (2017) in high-dimensional settings.

S.5 Another case when the quasi GPF test is more powerful than the L^2-norm based test

Now we present another case when the quasi GPF test is more powerful than the L^2-norm based test. Under (42) and (45) in the main paper, we further assume that for each

$i = 1, 2, \ldots, k$, we have

$$\varpi_i^0[(s_1, t_1), (s_2, t_2)] = \begin{cases} 1, & (s_1, t_1) = (s_2, t_2), \\ 1, & (s_1, s_2) = (t_2, t_1), \\ 2, & s_1 = t_1 = s_2 = t_2, \\ 0, & \text{otherwise}, \end{cases} \tag{S.1}$$

Assumption (S.1) describes the case when $\varpi_i^0[(s_1, t_1), (s_2, t_2)]$'s are dominated by the values on their diagonal surfaces. It is the case when the underlying processes $v_{i1}^0(t),\ i = 1, 2, \ldots, k$ are Gaussian white noises (see a proof later). Then under Assumptions A1 and A2, the local alternative (26) and the conditions (36), (45) and (S.1), by some tedious algebra, we have

$$\delta_{\bar{\varpi}}^4 = \frac{(k-1)^{-2}}{(b-a)^4}(\boldsymbol{d}^T \boldsymbol{W} \boldsymbol{d})^2 \left\{ \int_{\mathcal{T}^2} [h(s)h(t)]^{-2} \mathrm{d}s\mathrm{d}t \right\}^2, \ \ \delta^4 = (b-a)^4 (\boldsymbol{d}^T \boldsymbol{W} \boldsymbol{d})^2,$$

and

$$\mathrm{Var}(S_{\bar{\varpi}}) = \frac{2(k-1)^{-2}}{(b-a)^4} \boldsymbol{d}^T \boldsymbol{W} \boldsymbol{d} \int_{\mathcal{T}^2} [h(s)h(t)]^{-2} \mathrm{d}s\mathrm{d}t, \ \ \mathrm{Var}(\tilde{S}) = 2\boldsymbol{d}^T \boldsymbol{W} \boldsymbol{d} \int_{\mathcal{T}^2} [h(s)h(t)]^2 \mathrm{d}s\mathrm{d}t.$$

It follows that

$$\frac{2\delta_{\bar{\varpi}}^4}{\mathrm{Var}(S_{\bar{\varpi}})} = \boldsymbol{d}^T \boldsymbol{W} \boldsymbol{d} \int_{\mathcal{T}^2} [h(s)h(t)]^{-2} \mathrm{d}s\mathrm{d}t, \ \ \frac{2\delta^4}{\mathrm{Var}(\tilde{S})} = (b-a)^4 (\boldsymbol{d}^T \boldsymbol{W} \boldsymbol{d}) / \int_{\mathcal{T}^2} [h(s)h(t)]^2 \mathrm{d}s\mathrm{d}t.$$

Thus, $\delta_{\bar{\varpi}}^4 / \mathrm{Var}(S_{\bar{\varpi}}) > \delta^4 / \mathrm{Var}(\tilde{S})$ is equivalent to

$$\int_{\mathcal{T}^2} [h(s)h(t)]^{-2} \mathrm{d}s\mathrm{d}t \int_{\mathcal{T}^2} [h(s)h(t)]^2 \mathrm{d}s\mathrm{d}t > (b-a)^4,$$

which is always true by the Cauchy–Schwarz inequality provided that $h(t)$ is not a constant function.

On the Condition (S.1). We show that (S.1) holds when $v_{ij}^0(t),\ j = 1, 2, \ldots, n_i,\ i = 1, 2, \ldots, k$, are i.i.d. from a Gaussian white noise process, e.g., for any given t, $v_{ij}^0(t) \sim \mathcal{N}(0, 1)$ and for $s \neq t$, $v_{ij}^0(s)$ and $v_{ij}^0(t)$ are independent. Since $v_{ij}^0(t)$'s are Gaussian, we have (Zhang 2013, (10.13)),

$$\varpi_i^0[(s_1, t_1), (s_2, t_2)] = \gamma_i^0(s_1, s_2)\gamma_i^0(t_1, t_2) + \gamma_i^0(s_1, t_2)\gamma_i^0(s_2, t_1), \tag{S.2}$$

where $\gamma_i^0(s, t) = 1\{s = t\}$. There are only three cases where $\varpi_i^0[(s_1, t_1), (s_2, t_2)] \neq 0$:

1. When $(s_1, t_1) = (s_2, t_2)$ but $(s_1, s_2) \neq (t_2, t_1)$, the first term of the right-hand side of (S.2) is nonzero while the second term is zero, i.e.,

$$\varpi_i^0[(s_1, t_1), (s_2, t_2)] = \varpi_i^0[(s_1, t_1), (s_1, t_1)] = 1.$$

2. When $(s_1, s_2) = (t_2, t_1)$ but $(s_1, t_1) \neq (s_2, t_2)$, the first term of the right-hand side of (S.2) is zero but the second term is nonzero, i.e.,

$$\varpi_i^0[(s_1, t_1), (s_2, t_2)] = \varpi_i^0[(s_1, t_1), (t_1, s_1)] = 1.$$

3. When $(s_1, t_1) = (s_2, t_2)$ and $(s_1, s_2) = (t_2, t_1)$, both the terms are nonzero, i.e.,

$$\varpi_i^0[(s_1, t_1), (s_2, t_2)] = \varpi_i^0[(s_1, s_1), (s_1, s_1)] = 1 + 1 = 2.$$

□

APPENDIX: Technical Proofs

Lemma 1. *Under Assumptions A1–A3 and the null hypothesis (2), as $n \to \infty$, we have $\hat{\varpi}[(s_1, t_1), (s_2, t_2)] \xrightarrow{p} \varpi[(s_1, t_1), (s_2, t_2)]$ and $SSE(s, t)/(n - k) \xrightarrow{p} \varpi[(s, t), (s, t)]$ uniformly where $\varpi[(s_1, t_1), (s_2, t_2)]$ is given in (14).*

Proof. First of all, we show Assumption A2 implies

$$\rho_i = \sup_{t\in\mathcal{T}} \gamma_i(t,t) < \infty, \text{ and } \mathrm{E}\|v_{i1}\|^4 = \mathrm{E}\left[\int_{\mathcal{T}} v_{i1}^2(t)\mathrm{d}t\right]^2 < \infty, \ i = 1, 2, \ldots, k. \tag{A.3}$$

Assumption A2 implies $\sup_{s,t\in\mathcal{T}} \mathrm{E}[v_{i1}^2(s)v_{i1}^2(t)] = C_i < \infty$, where C_i is some finite number, $i = 1, 2, \ldots, k$. By Cauchy–Schwarz inequality,

$$\begin{aligned}\gamma_i(t,t) = \mathrm{E}[v_{i1}(t)v_{i1}(t)] &\leq \sqrt{\mathrm{E}[v_{i1}^2(t)v_{i1}^2(t)] \times \mathrm{E}(1^2)} \\ &\leq \sqrt{\sup_{s,t\in\mathcal{T}} \mathrm{E}[v_{i1}^2(s)v_{i1}^2(t)]} \leq \sqrt{C_i},\end{aligned}$$

and

$$\begin{aligned}&\mathrm{E}\left[\int_{\mathcal{T}} v_{i1}^2(t)\mathrm{d}t\right]^2 = \mathrm{E}\left[\int_{\mathcal{T}^2} v_{i1}^2(s)v_{i1}^2(t)\mathrm{d}s\mathrm{d}t\right] \\ =& \int_{\mathcal{T}^2} \mathrm{E}[v_{i1}^2(s)v_{i1}^2(t)]\mathrm{d}s\mathrm{d}t \leq \int_{\mathcal{T}^2} C_i\mathrm{d}s\mathrm{d}t = C_i(b-a)^2 < \infty,\end{aligned}$$

thus (A.3) is shown.

By (A.3), we have $v_{ij}(t) = O_p(1)$ and as $n \to \infty$, $\bar{v}_i(t) = o_p(1)$ uniformly for $t \in \mathcal{T}$, $j = 1, 2, \ldots, n_i$; $i = 1, 2, \ldots, k$. This is because we have $\mathrm{E}[v_{ij}(t)] = 0$, $\mathrm{Var}[v_{ij}(t)] = \gamma_i(t,t) \leq \rho_i < \infty$, $t \in \mathcal{T}$ and $\mathrm{E}[\bar{v}_i(t)] = 0$, $\mathrm{Var}[\bar{v}_i(t)] = \gamma_i(t,t)/n_i \leq \rho_i/n_i \to 0$, $t \in \mathcal{T}$ as $n \to \infty$. As $n \to \infty$, we have $\hat{v}_{ij}(s_1)\hat{v}_{ij}(t_1)\hat{v}_{ij}(s_2)\hat{v}_{ij}(t_2) = [v_{ij}(s_1) - \bar{v}_i(s_1)][v_{ij}(t_1) - \bar{v}_i(t_1)][v_{ij}(s_2) - \bar{v}_i(s_2)][v_{ij}(t_2) - \bar{v}_i(t_2)] = v_{ij}(s_1)v_{ij}(t_1)v_{ij}(s_2)v_{ij}(t_2) + o_p(1)$ uniformly for $s, t \in \mathcal{T}$; $j = 1, 2, \ldots, n_i$; $i = 1, 2, \ldots, k$. Under the null hypothesis (2) and by Theorems 10.4 and 10.6 in Zhang (2013), it is easy to show that $\hat{\gamma}_i(s,t) \xrightarrow{p} \gamma_i(s,t) = \gamma(s,t)$, $i = 1, 2, \ldots, k$ and $\hat{\gamma}(s,t) \xrightarrow{p} \gamma(s,t)$ uniformly. Therefore, as $n \to \infty$, we have

$$\begin{aligned}&n_i^{-1}\textstyle\sum_{j=1}^{n_i} \hat{v}_{ij}(s_1)\hat{v}_{ij}(t_1)\hat{v}_{ij}(s_2)\hat{v}_{ij}(t_2) - \hat{\gamma}(s_1,t_1)\hat{\gamma}(s_2,t_2) \\ \to\ & \mathrm{E}[v_{i1}(s_1)v_{i1}(t_1)v_{i1}(s_2)v_{i1}(t_2)] - \gamma(s_1,t_1)\gamma(s_2,t_2),\ i = 1, 2, \ldots, k,\end{aligned}$$

uniformly. By (15), we have

$$\begin{aligned}
& \hat{\varpi}\left[(s_1,t_1),(s_2,t_2)\right] \\
= \;& n^{-1}\sum_{i=1}^{k}\sum_{j=1}^{n_i}\hat{v}_{ij}(s_1)\hat{v}_{ij}(t_1)\hat{v}_{ij}(s_2)\hat{v}_{ij}(t_2) - \hat{\gamma}(s_1,t_1)\hat{\gamma}(s_2,t_2) \\
= \;& n^{-1}\sum_{i=1}^{k} n_i \left\{ n_i^{-1}\sum_{j=1}^{n_i}[\hat{v}_{ij}(s_1)\hat{v}_{ij}(t_1)\hat{v}_{ij}(s_2)\hat{v}_{ij}(t_2)] - \hat{\gamma}(s_1,t_1)\hat{\gamma}(s_2,t_2) \right\} \\
\to \;& \varpi[(s,t),(s,t)],
\end{aligned}$$

uniformly for all $s,t \in \mathcal{T}$. Similarly, we can get $\mathrm{SSE}(s,t)/(n-k) \xrightarrow{p} \varpi[(s,t),(s,t)]$. □

Proof of Theorem 1. Recall that $F_n(s,t) = \frac{\mathrm{SSB}_{(s,t)/(k-1)}}{\mathrm{SSE}_{(s,t)/(n-k)}}$. For any $s,t \in \mathcal{T}$, $\mathrm{SSB}(s,t)$ can be expressed as

$$\mathrm{SSB}(s,t) = \boldsymbol{z}_n(s,t)^T[\boldsymbol{I}_k - \boldsymbol{b}_n\boldsymbol{b}_n^T/(n-k)]\boldsymbol{z}_n(s,t), \tag{A.1}$$

where $\boldsymbol{z}_n(s,t) = [z_1(s,t), z_2(s,t), \ldots, z_k(s,t)]^T$, with

$$\begin{aligned}
z_i(s,t) &= \sqrt{n_i - 1}[\hat{\gamma}_i(s,t) - \gamma(s,t)],\ i = 1,2,\ldots,k, \\
\boldsymbol{b}_n &= (\sqrt{n_1-1}, \sqrt{n_2-1}, \ldots, \sqrt{n_k-1})^T.
\end{aligned}$$

Since $\boldsymbol{b}_n^T\boldsymbol{b}_n/(n-k) = 1$, it is easy to verify that $\boldsymbol{I}_k - \boldsymbol{b}_n\boldsymbol{b}_n^T/(n-k)$ is an idempotent matrix with rank $k-1$. In addition, as $n \to \infty$, we have

$$\boldsymbol{I}_k - \boldsymbol{b}_n\boldsymbol{b}_n^T/(n-k) \to \boldsymbol{W} = \boldsymbol{I}_k - \boldsymbol{b}\boldsymbol{b}^T, \text{with } \boldsymbol{b} = (\sqrt{\tau_1}, \sqrt{\tau_2}, \ldots, \sqrt{\tau_k})^T, \tag{A.2}$$

where $\tau_i, i = 1,2,\ldots,k$ are given in Assumption A1. Note that $\boldsymbol{I}_k - \boldsymbol{b}\boldsymbol{b}^T$ in (A.2) is also an idempotent matrix of rank $k-1$, which has the following singular value decomposition:

$$\boldsymbol{I}_k - \boldsymbol{b}\boldsymbol{b}^T = \boldsymbol{U}\begin{pmatrix} \boldsymbol{I}_{k-1} & \boldsymbol{0} \\ \boldsymbol{0}^T & 0 \end{pmatrix}\boldsymbol{U}^T, \tag{A.3}$$

where the columns of $\boldsymbol{U}$ are the eigenvectors of $\boldsymbol{I}_k - \boldsymbol{b}\boldsymbol{b}^T$.

Under the given conditions and by Theorem 10.4 of Zhang (2013), we have $\boldsymbol{z}_n(s,t) \xrightarrow{d} \boldsymbol{z}(s,t) \sim \mathrm{GP}_k(\boldsymbol{0}, \varpi \boldsymbol{I}_k)$ uniformly for all $s,t \in \mathcal{T}$ where $\varpi[(s_1,t_1),(s_2,t_2)]$ is given in (14). In addition, by Lemma 1, we have $\mathrm{SSE}(s,t)/(n-k) \xrightarrow{p} \varpi[(s,t),(s,t)]$ uniformly. Then by (A.2) and Slutsky's theorem, we have $F_n(s,t) \xrightarrow{p} (k-1)^{-1}\boldsymbol{z}(s,t)^T[\boldsymbol{I}_k - \boldsymbol{b}\boldsymbol{b}^T]\boldsymbol{z}(s,t)/\varpi[(s,t),(s,t)]$. Now by the singular value decomposition (A.3) of $\boldsymbol{I}_k - \boldsymbol{b}\boldsymbol{b}^T$, we have $F_n(s,t) \xrightarrow{p} (k-1)^{-1}\boldsymbol{\omega}(s,t)^T\boldsymbol{\omega}(s,t)$ where $\boldsymbol{\omega}(s,t) = (\boldsymbol{I}_{k-1}, \boldsymbol{0})\boldsymbol{U}^T\boldsymbol{z}(s,t)/\sqrt{\varpi[(s,t),(s,t)]} = [\omega_1(s,t), \omega_2(s,t), \ldots, \omega_{k-1}(s,t)]^T$ and $\boldsymbol{\omega}(s,t) \sim \mathrm{GP}_{k-1}(\boldsymbol{0}, \gamma_\varpi \boldsymbol{I}_{k-1})$ with $\gamma_\varpi[(s_1,t_1),(s_2,t_2)] = \varpi[(s_1,t_1),(s_2,t_2)]/\sqrt{\varpi[(s_1,t_1),(s_1,t_1)]\varpi[(s_2,t_2),(s_2,t_2)]}$. It follows that $F_n(s,t) \xrightarrow{p} (k-1)^{-1}\sum_{i=1}^{k-1}\omega_i^2(s,t)$. Since $T_n = (b-a)^{-2}\int_{\mathcal{T}^2} F_n(s,t)\mathrm{d}s\mathrm{d}t$ and $F_{\max} = \sup_{s,t\in\mathcal{T}} F_n(s,t)$, the second expression of (18) is shown by the continuous mapping theorem for random elements taking values in a Hilbert space (Billingsley 1999, p.20; Cuevas et al. 2004) and along the same lines as the proof of Theorem 4.10 of Chapter 4 in Zhang (2013) (p.90). The expression (19) can be obtained similarly following the proof of Theorem 1 of Guo et al. (2018). □

Proof of Theorem 2. By Lemma 1, we have $\hat{\varpi}[(s_1,t_1),(s_2,t_2)] \xrightarrow{p} \varpi[(s_1,t_1),(s_2,t_2)]$. It follows that $\hat{\gamma}_\varpi[(s_1,t_1),(s_2,t_2)] \xrightarrow{p} \gamma_\varpi[(s_1,t_1),(s_2,t_2)]$ and then $\mathrm{tr}(\hat{\gamma}_\varpi^{\otimes 2}) \xrightarrow{p} \mathrm{tr}(\gamma_\varpi^{\otimes 2})$ follow immediately from the continuous mapping theorem for random elements taking values in a Hilbert space. Therefore, as $n \to \infty$, we have $\hat{d} \xrightarrow{p} d$. It then follows that $\hat{C}_\alpha \xrightarrow{p} \tilde{C}_\alpha$. □

Proof of Theorem 3. Notice that for any $s,t \in \mathcal{T}$, $\mathrm{SSB}(s,t) = \boldsymbol{z}_n(s,t)^T[\boldsymbol{I}_k - \boldsymbol{b}_n\boldsymbol{b}_n^T/(n-k)]\boldsymbol{z}_n(s,t)$, where $\boldsymbol{z}_n(s,t) = [z_1(s,t), z_2(s,t), \ldots, z_k(s,t)]^T$ with $z_i(s,t) = \sqrt{n_i - 1}[\hat{\gamma}_i(s,t) - \gamma_i(s,t)] + \sqrt{n_i-1}[\gamma_i(s,t) - \gamma(s,t)]$, $i = 1, 2 \ldots, k$. Applying Theorem 10.4 of Zhang (2013), we have $\sqrt{n_i-1}[\hat{\gamma}_i(s,t) - \gamma_i(s,t)] \xrightarrow{d} \mathrm{GP}(0, \varpi_i)$, $i = 1, 2, \ldots, k$. By the alterna-

tive hypothesis (26), we also have $\sqrt{n_i-1}[\gamma_i(s,t)-\gamma(s,t)]=d_i(s,t)$, where the functions $d_i(s,t),\ i=1,2,\ldots,k\in\mathcal{L}^2(\mathcal{T}^2)$ and $\mathcal{T}^2=[a,b]\otimes[a,b]$. It follows that $\boldsymbol{z}_n(s,t)\xrightarrow{d}\boldsymbol{z}_1(s,t)+\boldsymbol{d}(s,t)\sim \mathrm{GP}_k[\boldsymbol{d},\mathrm{diag}(\varpi_1,\varpi_2,\ldots,\varpi_k)]$, where $\boldsymbol{z}_1(s,t)\sim \mathrm{GP}_k[\boldsymbol{0},\mathrm{diag}(\varpi_1,\varpi_2,\ldots,\varpi_k)]$ and $\boldsymbol{d}(s,t)=[d_1(s,t),d_2(s,t),\ldots,d_k(s,t)]^T$.

Similar to the proof of Lemma 1 and under the local alternative hypothesis (26), as $n\to\infty$, we have $\mathrm{SSE}(s,t)/(n-k)\xrightarrow{p}\bar{\varpi}[(s,t),(s,t)]=\sum_{i=1}^k\tau_i\varpi_i[(s,t),(s,t)]$ uniformly for all $s,t\in\mathcal{T}$. Since $\mathcal{T}$ is a finite interval and $F_n(s,t)$ is equicontinuous over $\mathcal{T}$, by Slusky's theorem and Theorem 2.1 of Newey (1991), we can show that as $n\to\infty$, we have $F_{\max}\xrightarrow{d}F_1$ with

$$\begin{aligned}F_1 &= (k-1)^{-1}\sup_{s,t\in\mathcal{T}}\left\{[\boldsymbol{z}_1(s,t)+\boldsymbol{d}(s,t)]^T\boldsymbol{W}[\boldsymbol{z}_1(s,t)+\boldsymbol{d}(s,t)]/\bar{\varpi}[(s,t),(s,t)]\right\}\\ &= (k-1)^{-1}\sup_{s,t\in\mathcal{T}}\left\{[\boldsymbol{z}_1(s,t)^T\boldsymbol{W}\boldsymbol{z}_1(s,t)+2\boldsymbol{z}_1(s,t)^T\boldsymbol{W}\boldsymbol{d}(s,t)+\boldsymbol{d}(s,t)^T\boldsymbol{W}\boldsymbol{d}(s,t)]\right.\\ &\quad\left.\times\bar{\varpi}^{-1}[(s,t),(s,t)]\right\},\end{aligned}$$

where the idempotent matrix $\boldsymbol{W}$ is defined in (A.2). By the continuous mapping theorem for random elements taking values in a Hilbert space again, we can easily get $T_n\xrightarrow{d}T_1$ with

$$T_1\overset{d}{=}\frac{(k-1)^{-1}}{(b-a)^2}\int_{\mathcal{T}^2}[\boldsymbol{z}_1(s,t)^T\boldsymbol{W}\boldsymbol{z}_1(s,t)+2\boldsymbol{z}_1(s,t)^T\boldsymbol{W}\boldsymbol{d}(s,t)+\delta^2(s,t)]/\bar{\varpi}[(s,t),(s,t)]\mathrm{d}s\mathrm{d}t.$$

□

Proof of Theorem 4. By Theorem 3, we have $T_1\overset{d}{=}T_{0\bar{\varpi}}+2S_{\bar{\varpi}}+\delta^2_{\bar{\varpi}}$, where

$$\begin{aligned}T_{0\bar{\varpi}} &= \tfrac{(k-1)^{-1}}{(b-a)^2}\textstyle\int_{\mathcal{T}^2}\boldsymbol{z}_1(s,t)^T\boldsymbol{W}\boldsymbol{z}_1(s,t)/\bar{\varpi}[(s,t),(s,t)]\mathrm{d}s\mathrm{d}t,\\ S_{\bar{\varpi}} &= \tfrac{(k-1)^{-1}}{(b-a)^2}\textstyle\int_{\mathcal{T}^2}\boldsymbol{z}_1(s,t)^T\boldsymbol{W}\boldsymbol{d}(s,t)/\bar{\varpi}[(s,t),(s,t)]\mathrm{d}s\mathrm{d}t,\\ \delta^2_{\bar{\varpi}} &= \tfrac{(k-1)^{-1}}{(b-a)^2}\textstyle\int_{\mathcal{T}^2}\boldsymbol{d}(s,t)^T\boldsymbol{W}\boldsymbol{d}(s,t)/\bar{\varpi}[(s,t),(s,t)]\mathrm{d}s\mathrm{d}t.\end{aligned}$$

Let

$$\gamma_{\bar{\varpi}i}[(s_1,t_1),(s_2,t_2)]=\varpi_i[(s_1,t_1),(s_2,t_2)]/\sqrt{\bar{\varpi}[(s_1,t_1),(s_1,t_1)]\bar{\varpi}[(s_2,t_2),(s_2,t_2)]},\ i=1,2,\ldots,k.$$

Since $\mathrm{tr}(\sum_{i=1}^{k} \tau_i \gamma_{\bar{\varpi} i}) = (b-a)^2$, we have $\mathrm{tr}(\gamma_{\bar{\varpi} i}) < \infty, i = 1, 2, \ldots, k$. In addition, since $\boldsymbol{W}$ is an idempotent matrix, its eigenvalues are either 0 or 1. It follows that

$$|T_{0\bar{\varpi}}| \leq \frac{(k-1)^{-1}}{(b-a)^2} \int_{\mathcal{T}^2} \boldsymbol{z}_1(s,t)^T \boldsymbol{z}_1(s,t) / \bar{\varpi}[(s,t),(s,t)] \mathrm{d}s\mathrm{d}t \stackrel{d}{=} \frac{(k-1)^{-1}}{(b-a)^2} \sum_{i=1}^{k} \sum_{r=1}^{\infty} \lambda_{ir} A_{ir}, \tag{A.4}$$

where $A_{ir} \overset{i.i.d.}{\sim} \chi_1^2$ and for each $i = 1, 2, \ldots, k$, λ_{ir}'s are the eigenvalues of $\gamma_{\bar{\varpi} i}[(s_1,t_1),(s_2,t_2)]$. It follows that $T_{0\bar{\varpi}}$ is a proper random variable with finite mean and variance. By the Cauchy–Schwarz inequality, we have $|S_{\bar{\varpi}}| \leq T_{0\bar{\varpi}}^{1/2} \delta_{\bar{\varpi}}$. Then $T_1 = O_p(\delta_{\bar{\varpi}}) + \delta_{\bar{\varpi}}^2$. It follows that as $\delta_{\bar{\varpi}} \to \infty$, we have $\Pr(T_1 \geq C_\alpha) \to 1$. Under the given conditions and Theorem 3, $\Pr(T_n \geq C_\alpha) \to \Pr(T_1 \geq C_\alpha) \to 1$. □

Proof of Theorem 5. By (30), we first have $\Pr(F_{\max} \geq C_{2\alpha}^*) \geq \Pr(T_n \geq C_{2\alpha}^*)$. It follows that as $\delta_{\bar{\varpi}} \to \infty$, we can show that $\Pr(T_n \geq C_{2\alpha}^*) \to 1$, following the proof of Theorem 4. The assertion $\Pr(F_{\max} \geq C_{2\alpha}^*) \to 1$ also follows immediately. □

References

Billingsley, P. (1999). *Convergence of Probability Measures*. John Wiley & Sons, 2nd edition.

Carey, J. R., Papadopoulos, N. T., Müller, H.-G., Katsoyannos, B. I., Kouloussis, N. A., Wang, J.-L., Wachter, K., Yu, W., and Liedo, P. (2008). Age structure changes and extraordinary lifespan in wild medfly populations. *Aging Cell*, 7(3):426–437.

Cuevas, A., Febrero, M., and Fraiman, R. (2004). An anova test for functional data. *Computational Statistics & Data Analysis*, 47(1):111–122.

Guo, J., Zhou, B., and Zhang, J.-T. (2016). A further study of an L^2-norm based test for the equality of several covariance functions. Manuscript.

Guo, J., Zhou, B., and Zhang, J.-T. (2018). A supremum-norm based test for the equality of several covariance functions. *Computational Statistics & Data Analysis*, 124:15–26.

Newey, W. K. (1991). Uniform convergence in probability and stochastic equicontinuity. *Econometrica: Journal of the Econometric Society*, 59(4):1161–1167.

Satterthwaite, F. E. (1946). An approximate distribution of estimates of variance components. *Biometrics*, 2(6):110–114.

Welch, B. L. (1947). The generalization of 'Student's' problem when several different population variances are involved. *Biometrika*, 34(1/2):28–35.

Zhang, J.-T. (2005). Approximate and asymptotic distributions of chi-squared–type mixtures with applications. *Journal of the American Statistical Association*, 100(469):273–285.

Zhang, J.-T. (2013). *Analysis of Variance for Functional Data*. CRC Press.

Zhang, J.-T., Guo, J., Zhou, B., and Cheng, M. (2017). A simple and adaptive two-sample test in high-dimensions based on L^2 norm. Manuscript.